

# CrystEngComm

Accepted Manuscript



This is an *Accepted Manuscript*, which has been through the Royal Society of Chemistry peer review process and has been accepted for publication.

*Accepted Manuscripts* are published online shortly after acceptance, before technical editing, formatting and proof reading. Using this free service, authors can make their results available to the community, in citable form, before we publish the edited article. We will replace this *Accepted Manuscript* with the edited and formatted *Advance Article* as soon as it is available.

You can find more information about *Accepted Manuscripts* in the [Information for Authors](#).

Please note that technical editing may introduce minor changes to the text and/or graphics, which may alter content. The journal's standard [Terms & Conditions](#) and the [Ethical guidelines](#) still apply. In no event shall the Royal Society of Chemistry be held responsible for any errors or omissions in this *Accepted Manuscript* or any consequences arising from the use of any information it contains.

## ARTICLE

## Implication of microstructure on mechanical behaviour of aspirin-paracetamol eutectic mixture

Cite this: DOI: 10.1039/x0xx00000x

Hemant Jain<sup>a</sup>, Kailas S. Khomane<sup>a</sup> and Arvind K. Bansal<sup>a</sup>

Received 00th May 2014,

Accepted 00th May 2014

DOI: 10.1039/x0xx00000x

[www.rsc.org/](http://www.rsc.org/)

The present work investigates the mechanical behaviour of aspirin-paracetamol (ASP-PCM) eutectic mixture (EM). EM of ASP-PCM was prepared using solvent evaporation method. Differential scanning calorimetry (DSC) and powder X-ray diffraction (PXRD) confirmed eutectic formation at the composition of 53:47 (ASP:PCM). Compaction behaviour of EM and physical mixture (PM) of ASP and PCM was compared using a fully instrumented rotary tablet press equipped with Portable Press Analyzer™ (PPA). The obtained data were compared for compressibility, tableability and compactibility profiles and Heckel analysis. EM exhibited higher compressibility, tableability and plastic deformation as compared to PM. Heckel analysis showed the lower  $P_y$  (46.9 MPa) for EM as compared to PM (222.8 MPa), thus confirming better plastic deformation of EM. The better deformation behaviour of EM was attributed to its layered microstructure. Sliding of the adjacent layer over each other under applied compaction pressure offered higher plastic deformation and thus provided greater interparticulate bonding area in EM as compared to PM. However there was no significant difference in the compactibility profiles indicating similar interparticulate bonding strength of the two powders. Thus, EM showed better tableability compared to PM by virtue of its greater compressibility and plastic deformation.

### Introduction

Compaction is the most commonly used unit process in pharmaceutical industry. Initial stage of compaction involves particle rearrangement which is followed by further volume reduction by virtue of elastic deformation. After a critical point called as 'yield point', material starts to deform plastically.<sup>1</sup> Elastic deformation is reversible upon the release of the compaction load while plastic deformation is an irreversible process. Some materials undergo extensive fragmentation under the applied compaction pressure called as brittle fracture. Fragmented particles further undergo the elastic or plastic deformation.

A model based on bonding area-bonding strength (BABS) has been proposed to explain compaction.<sup>2</sup> According to this model tablet tensile strength or tableability is governed by interparticulate bonding area (BA) and bonding strength (BS).<sup>2</sup> Mechanical properties like elastic deformation, plastic deformation or brittle fracture influence the interparticulate bonding area. Crystallographic features like slip planes contribute to the interparticulate bonding area.

Slip planes in the crystal lattice allow easier slip, enabling greater plasticity, and hence produce stronger tablets. Interparticulate bonding strength is governed by interparticulate molecular forces like van der Waals forces. Thus, the factors those contribute to BABS govern the tableability.

Eutectic mixture (EM) is a mixture of two components that are completely miscible in the liquid state but immiscible in the solid state. Thermodynamically such systems can be considered as intimately blended physical mixtures (PM).<sup>3, 4</sup> The melting point of the EM is lower than the melting point of either component.<sup>5, 6</sup> The increased surface area for the components is mainly responsible for the increased dissolution rate of sparingly water soluble drug.<sup>5</sup> These components crystallize simultaneously in a particulate size and are held together by means of non bonding interaction (NBIs).

The present work investigates the mechanical behaviour of pharmaceutical eutectic systems. Eutectic systems that consist of lamellar microstructures, are crystallized as side by side planes and are expected to behave like slip planes of the crystal lattice.<sup>7</sup> Hence it was hypothesized that microstructure of eutectic system may contribute to greater plastic deformation under the applied compaction pressure, thus affecting tableability. Aspirin-paracetamol eutectic system offers these

<sup>a</sup>Department of Pharmaceutics, National Institute of Pharmaceutical Education and Research (NIPER), S.A.S. Nagar, Punjab-160 062, India  
E-mail: akbansal@niper.ac.in

## ARTICLE

CrystEngComm

crystallographical features and was hence selected as a model materials. Compaction studies were performed using a fully instrumented rotary tablet press and data were compared for compressibility, tableability and compactibility profile and Heckel analysis. Microstructure was characterized using various thermal and spectroscopic techniques and was correlated to its mechanical behaviour. EM of Aspirin-Paracetamol (ASP-PCM) was compared to their PM using compressibility, compactibility, tableability and Heckel analysis.

## Materials and Methods

### Material

Aspirin was purchased from Allwell Pharmaceuticals Co., Chandigarh. Paracetamol was gifted by Arbro Pharmaceuticals Ltd., New Delhi.

### Generation of EM

EM was generated by solvent evaporation method. Different proportion of aspirin and paracetamol was dissolved in methanol: dichloromethane (DCM) (3:1) solution. From this solution, solvent evaporated by Buchi Rotavapour® at 50 °C, 130-150 rpm and vacuum <10 mbar. PM prepared by taking appropriate concentration of both ASP and PCM.

### Powder X-ray diffraction (PXRD)

PXRD patterns of samples were recorded at room temperature on a Bruker's D8 Advance diffractometer (Bruker AXS, Karlsruhe, West Germany) with Cu  $K\alpha$  radiation (1.54 Å), at 40 kV, 40 mA passing through a nickel filter. Analysis was performed in a continuous mode with a step size of 0.01° and step time of 1 s over an angular range of 3–40°  $2\theta$ . Obtained diffractograms were analysed with DIFFRAC plus EVA, version 9.0 (Bruker AXS, Karlsruhe, West Germany) diffraction software.

### Differential scanning calorimetry (DSC)

Melting temperature and heat of fusion were determined using DSC, Model Q2000 (TA Instruments, New Castle, DE). Prior to analysis, the instrument was calibrated using a high purity standard of indium for temperature (156.58 °C) and heat flow (28.71 J/g) measurement, respectively. Accurately weighed samples of about 3.5 to 4.5 mg were analysed using  $T_{zero}$  aluminium pans, in temperature range of 25 to 200 °C at a heating rate of 10 °C/min. Dry nitrogen purge was maintained at 50 mL/min.

### Optical and polarized microscopy

Samples were mounted on glass slides and observed under optical as well as polarized light. Birefringence was observed under the polarized light. Leica DMLP polarized light microscope (Leica Microsystems, Wetzlar, GmbH, Germany), equipped with Linkam LTS 350 hot stage. Photomicrographs

were acquired using JVS color video camera and analyzed using Linksys32 software.

### Moisture content

Moisture content was determined by Karl Fischer (KF) titration (Metrohm 794 Basic Titrino, Switzerland). The instrument was calibrated with disodium tartrate dihydrate for accuracy of moisture determination. Sample size of approximately 300 mg was utilized for the determination of moisture content ( $n = 3$ ).

### True density and flow properties

The true density of both mixtures was determined in triplicate by helium pycnometry (Pycno 30, Smart Instruments, Mumbai, India) at  $25 \pm 2$  °C/ $40 \pm 5$  % RH. Bulk density and tapped density ( $n=3$ ) of the samples was determined by bulk density apparatus (ETD 1020, Electrolab, Mumbai, India) using USP method I. Flow properties of the materials were determined by calculating Hausner ratio and Carr's index.

### Specific surface area measurement

Specific surface area of both the mixtures was determined using nitrogen gas sorption (SMART SORB 91 Surface Area analyzer; Smart Instruments, Mumbai, India). The instrument was calibrated by injecting a known quantity of nitrogen. The measured parameters were then used to calculate the surface area of the sample by employing the adsorption theories of Brunauer, Emmett, and Teller (BET). An accurately weighed amount of sample was placed into the glass loop of the instrument and then submerged into liquid nitrogen. The quantity of the adsorbed gas was measured using thermal conductivity detector and then integrated using electronic circuit.

### Particle size distribution

Similar particle size fraction of ASP, PCM, PM and EM was obtained by sieving (60-120  $\mu\text{m}$ ).  $D_{50}$  and  $D_{90}$  of each fraction were determined by optical microscopy by measuring diameter along the longest axis, for at least 150 particles (DMLP microscope, Leica Microsystems, Wetzlar, Germany).

### Scanning electron microscopy (SEM)

Particle morphology of both forms was studied using a scanning electron microscope (S-3400, Hitachi Ltd., Tokyo, Japan) operated at an excitation voltage of 15 kV. Powders were mounted onto steel stage using double sided adhesive tape and coated with gold using ion sputter (E-1010, Hitachi Ltd., Japan).

### Confocal laser scanning microscopy (CLSM)

Microstructure of EM was visualised under CLSM (Olympus FV 1000 USA). Sample was mounted on the slide and observed under microscope.

### Tableting and data acquisition

A rotary tablet press (Mini II, Rimek, Ahmedabad, India) was equipped at one of the 8 stations with 8 mm D-tooling with flat punch tip. Feed frame was used for uniform die filling and blind dies were used at all other positions. Precompression rollers were set out of function. Tablets of each material were compressed at constant volume. Humidity ( $40 \pm 2\%$  RH) and temperature ( $25 \pm 2$  °C) conditions were monitored throughout the study. Tablet weight was kept at  $200 \pm 5$  mg and applied force was levelled by moving the pressure roller with a hand wheel. Each powder was compacted at different compaction pressures on an instrumented rotary tablet press ranging from around 25 to 300 MPa. The tableting speed was kept constant at 14.0 rpm.

Data were acquired by Portable Press Analyzer™ (PPA) version 1.2, revision D (Data Acquisition and Analyzing System, PuuMan Oy, Kuopio, Finland), through an infrared telemetric device with 16-bit analog-to-digital converter (6 kHz). Force was measured by strain gauges at upper and lower punches ( $350\times$ , full Wheatstone bridge; I. Holland Tableting Science, Nottingham, U.K.), which were coupled with displacement transducers (linear potentiometer,  $1000\times$ ). Upper and lower punch data were recorded and transmitted on separate channels by individual amplifiers (“Boomerangs”). The amplifiers truncated the raw data from 16 bit to 12 bit after measuring to check IR transmission (data transmission rate, 50 kbd; internal data buffer, 1024 measurement points). Analysis of compaction data was carried out by PPA Analyze software (version 1.2, revision D). Accuracy of force and displacement transducers were 1% and 0.02%, respectively. The suitability of the data acquisition system has been reported in the literature.<sup>8-10</sup>

### Calculation of tablet tensile strength and porosity

Breaking force of the tablets was measured using a tablet hardness tester (tablet hardness tester, Erweka, USA). Tablet dimensions were measured using a digital caliper (Digimatic Mitutoyo Corporation, Japan). Tensile strength was calculated using eq. 1 to eliminate the undesirable effect of variable tablet thickness on measured breaking force.

$$\sigma = 2F/\pi dt \quad (1)$$

where  $\sigma$  is the tensile strength (MPa),  $F$  is the observed breaking force (N),  $d$  is the diameter (mm), and  $t$  is the thickness of the compact (mm).

The porosity,  $\varepsilon$  of the tablets was calculated by eq. 2,

$$\varepsilon = 1 - \rho_c/\rho_t \quad (2)$$

where  $\rho_c$  is the density of the tablet calculated from the weight and volume of the resulting tablet.  $\rho_t$  is the true density of powder.

### Statistical analysis

Statistical significance for values of various compaction parameters were compared using a two-tailed paired t-test (SigmaStat version 3.5, San Jose, CA, USA), and the test was considered to be statistically significant if  $P < 0.05$ .

## Results

### Screening for eutectic composition

Fig. 1 shows DSC overlay of generated mixtures of different proportion of ASP-PCM.

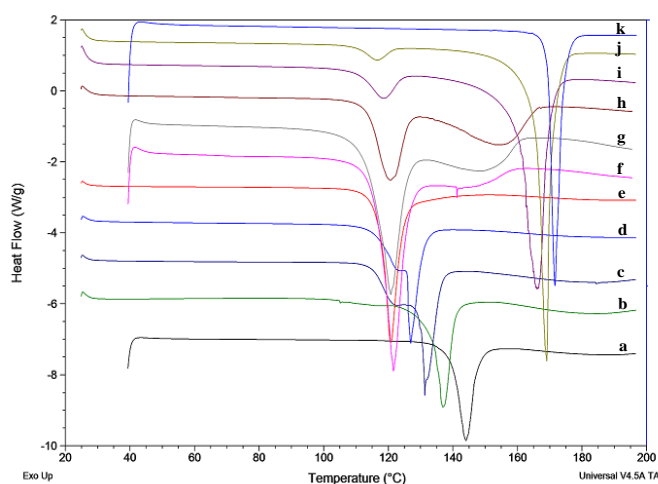


Fig. 1 DSC overlay for screening of eutectic composition. Key: ratio of aspirin:paracetamol (%w/w) was (a) 100:0 (b) 95:5 (c) 90:10 (d) 63:37 (e) 53:47 (f) 45:55 (g) 37:63 (h) 25:75 (i) 10:90 (j) 5:95 (k) 0:100.

All mixtures of ASP and PCM containing 5-37% w/w of PCM showed two endothermic events (Fig.1a-d). A single endothermic event was observed at 120.73 °C (Fig. 1e), when PCM concentration reached 47% w/w. Above 47% w/w PCM (Fig. 1f-j), again two endothermic events were observed. From Fig. 1, it can be concluded that eutectic system was formed at 53:47% w/w of ASP and PCM concentration, respectively. This correlated well with previous reports.<sup>11, 12</sup>

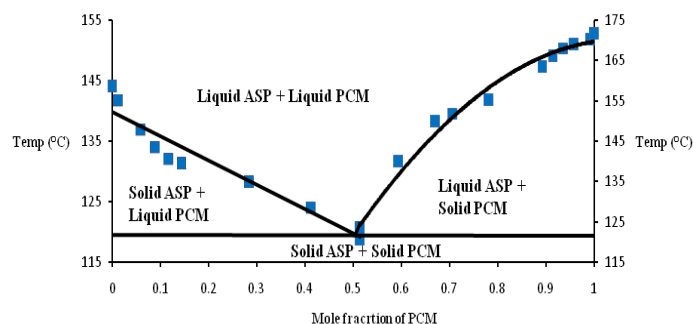


Fig. 2 Phase diagram of EM of ASP-PCM.

Binary phase diagram was constructed from melting values obtained during heating cycle of the generated mixtures (Fig. 2). Binary phase diagram suggested formation of EM at molar

## ARTICLE

ratio of 0.49:0.51 of ASP:PCM. Thus, eutectic system consists of ASP and PCM in 1:1 molar ratio. This system gave a eutectic temperature of 120.73 °C which is consistent with earlier reports.<sup>11</sup>

### Solid state characterization

The screening of eutectic composition confirmed, eutectic formation at 53:47% w/w of ASP and PCM concentrations respectively. This system gave one sharp endothermic peak at 120.73 °C. PM was prepared by taking 53:47% w/w of ASP and PCM and it was characterized using DSC. Fig. 3 shows DSC overlays of ASP, PCM, PM and EM.

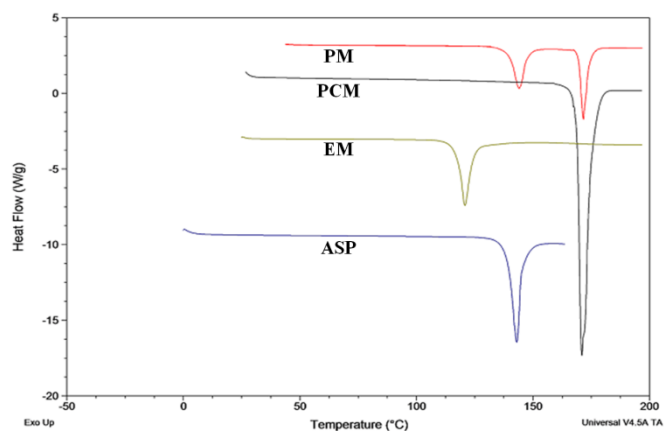


Fig. 3 DSC overlay of ASP, PCM, PM and EM.

The DSC tracing of ASP showed a single melting endotherm with a peak at 144.09 °C. PCM showed a sharp melting endotherm at 171.63 °C. Both values are in close agreement to earlier reports.<sup>13, 14</sup> PM showed melting of both ASP and PCM. In contrast EM showed single melting endothermic peak at 120.73 °C.

Generation of EM at 53:47% w/w was further supported by PXRD. Fig. 4 shows PXRD overlay of ASP, PCM, PM and EM. The diffraction pattern and the main diffraction angles of ASP and PCM agreed with the data of ASP form I<sup>15</sup> and PCM form I<sup>14</sup> from a previous study. PXRD pattern of EM was essentially remained same as PM. This was expected because of additive properties of eutectic components in PXRD (Fig. 4).

**Table 1** Melting point, heat of fusion, true density and moisture content of ASP, PCM, PM and EM.

Sample	Melting point (°C)	Heat of fusion (J/g)	True density <sup>a</sup> (g/cm <sup>3</sup> )	Moisture content (%)
ASP	144.09	93.19	1.43 (0.02)	0.08%
PCM	171.63	105.3	1.32 (0.03)	0.19%
PM	144.09, 171.63	49.19, 49.49	1.380 (0.03)	0.13%
EM	120.73	138.2	1.371 (0.02)	0.17%

<sup>a</sup>Standard deviations in parentheses

Table 1 summarizes the melting point, heat of fusion, true density, and moisture content data for individual drugs, PM and EM.

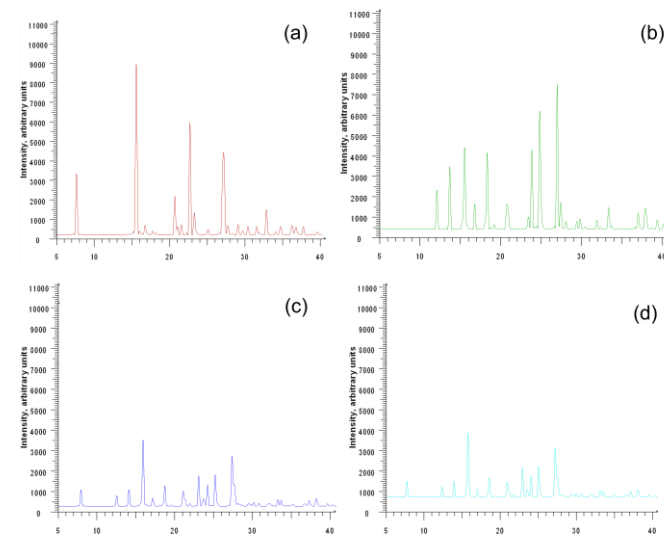


Fig. 4 XRD patterns of PCM, ASP, PM and EM.

### Physical characterization of mixtures

Good flow properties are a prerequisite for the assessment of the compaction behaviour using a fully instrumented rotary tablet press. Both the powders showed good flow properties, as indicated by Carr's index and Hausner ratio (Table 2). The effect of particle properties was reduced by keeping the particle shape and particle size distribution similar for ASP, PCM, PM and EM. Table 3 shows similar particle size distribution and specific surface area for PM and EM. SEM photograph showed similar particle shape of the two mixtures (Fig. 5).

**Table 2** Physical properties of EM and PM

Sample	Specific surface area (m <sup>2</sup> /gm)	Bulk density (g/cm <sup>3</sup> )	Tapped density (g/cm <sup>3</sup> )	Hausner ratio	Carr's index	Flowability*
PM	0.465	0.65	0.75	1.15	13.043	Good
EM	0.468	0.67	0.80	1.20	16.67	Fair

\*As per US Pharmacopeia general chapter 1174

**Table 3** Particle size distribution for ASP, PCM, PM and EM

Particle size distribution	ASP	PCM	PM	EM
D <sub>50</sub> (μm)	76	69	71	76
D <sub>90</sub> (μm)	99	105	103	101

### Microstructure characterization

EM was crystallized out as a thin layer on the glass slide and visualized using SEM and CLSM. Both the techniques suggested the formation of lamellar microstructure (Fig. 6 a, b).

SEM photograph of a Cross-section of EM particle further confirmed the presence of lamellar micro-structure (Fig 6c)

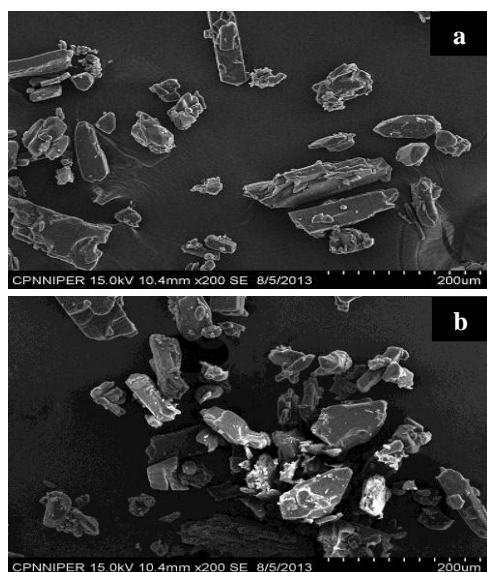


Fig. 5 SEM image of (a) PM (b) EM.

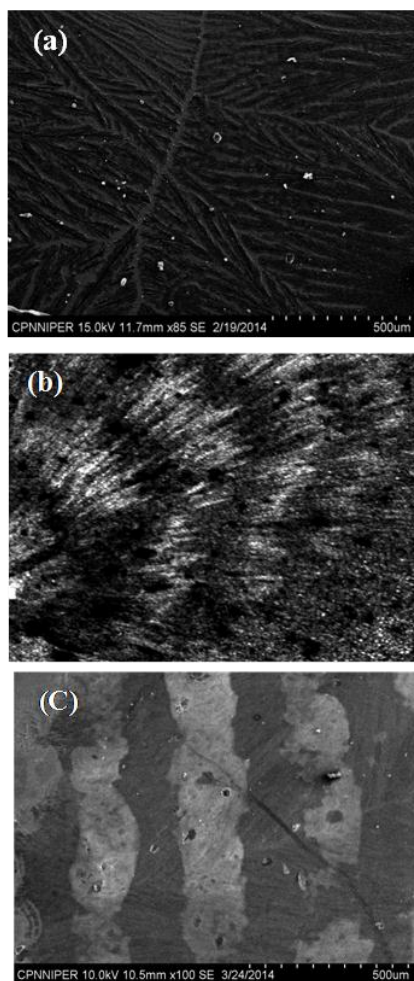


Fig. 6 Lamellar microstructure as visualized using (a) SEM and (b) CLSM (c) SEM photograph of a cross-sectioned EM particle

## Compaction behaviour of physical mixture and eutectic mixture

Preliminary experiments were carried out at very high compaction pressure (900 MPa) to rule out the possibility of polymorphic transformation during compaction study. Both mixtures were found to be stable and no polymorphic transformation was observed.

### Tabletability

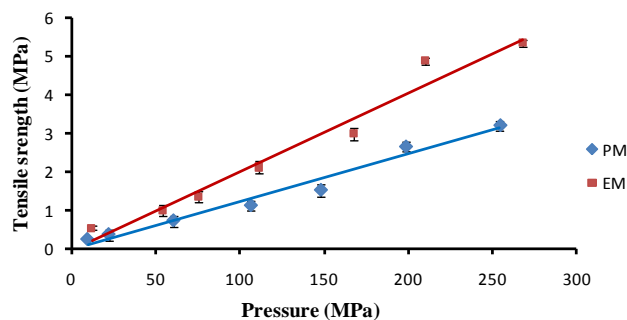


Fig. 7 Tabletability plot of EM and PM.

### CTC PROFILE

Tabletability is defined as the capacity of the powder material to be transformed into a tablet of specified strength under the effect of compaction pressure.<sup>2</sup> Fig. 7 shows the tabletability plot for EM and PM. Tensile strength of both mixtures increased with compaction pressure. However, EM showed higher tensile strength over PM at all compaction pressures. Thus, EM showed increased tabletability as compared to PM. Tabletability plot of EM and PM showed that tensile strength difference between EM and PM widens as pressure increased. At 50 MPa and 200 MPa pressure, tensile strength of EM and PM was found 0.99 MPa, 4.10 MPa and 0.60 MPa, 2.45 MPa, respectively.

### Compressibility

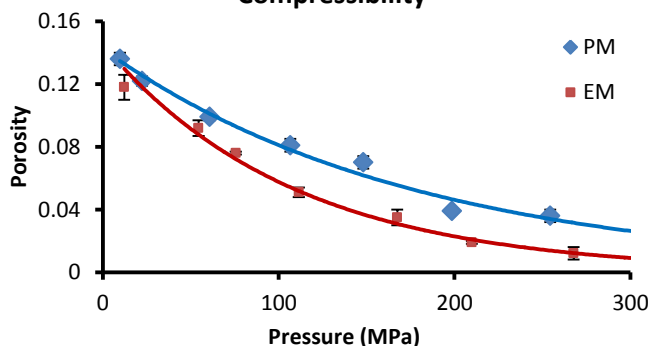


Fig. 8 Compressibility plot of EM and PM.

The compressibility of the material is its ability to be reduced in volume as a result of an applied pressure and is represented by a plot of tablet porosity against pressure.<sup>2</sup> A compressibility plot has been reported to represent the interparticulate bonding

## ARTICLE

area. EM exhibited greater compressibility as compared to the PM at a given compaction pressure (Fig. 8). Compressibility plot of EM and PM showed that porosity difference between EM and PM widen as pressure increased. At 50 MPa and 200 MPa pressure, porosity of EM and PM was found 0.088, 0.026 and 0.108, 0.052 respectively.

Compactibility is the ability of the material to produce tablets with sufficient strength under the effect of densification and is represented by a plot of tensile strength against tablet porosity.<sup>2</sup> Thus it shows the tensile strength of tablets normalized by tablet porosity. Both EM and PM exhibited similar compactibility, indicating their similar tensile strength at a given porosity (Fig. 9).

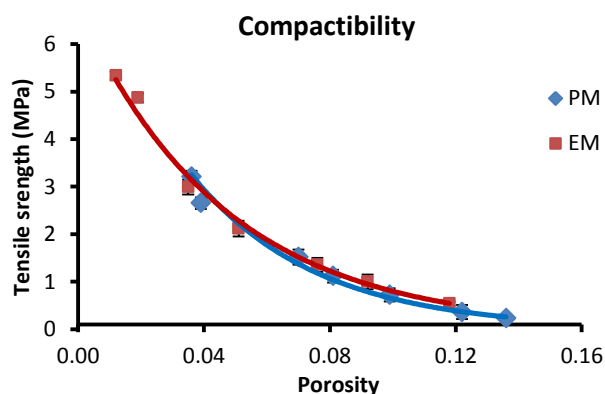


Fig. 9 Compactibility plot of EM and PM.

## HECKEL ANALYSIS

The Heckel equation transforms force and displacement data to a linear relationship for the materials undergoing compaction.<sup>16</sup> The basis for the equation is that densification of the bulk powder under pressure follows first-order kinetics.<sup>17</sup> It presents compaction data in term of its relative density under applied pressure. The Heckel equation expressed in the eq. 3

$$\ln [1/1-D] = KP + A \quad (3)$$

where D is the relative density of the tablet at applied pressure P and K is the slope of the straight line portion of the Heckel plot. Reciprocal transformation of the slope (K) gives mean yield pressure,  $P_y$ , which is related to the yield strength of the material.<sup>18</sup>

Densification behaviour of both mixtures were studied using Heckel analysis. Apparent mean yield pressure ( $P_y$ ) was calculated from the linear portions of the Heckel plot ( $R^2 > 0.98$  in all cases). Heckel analysis showed the lower  $P_y$  (46.9 MPa) for EM as compared to PM (222.8 MPa), thus confirming better plastic deformation of EM (Fig. 10).

## CrystEngComm

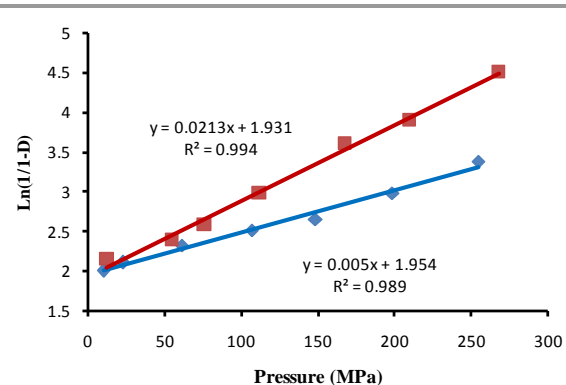


Fig. 10 Heckel plot of EM and PM.

## Discussion

The degree of interparticulate bonding (bonding area) and bond strength (bonding strength per unit area) determines the final quality of the tablets express as its tableability. Tableability is ability of the material to convert to a tablet of adequate mechanical strength and is governed by both compressibility and compactibility. The extent of bonding area can be obtained from the compressibility plots, whereas the bonding strength per unit bonding area is obtained from the compactibility plot. Collectively both parameters contribute to the quality of the tablets given by tableability.<sup>19</sup>

Presence of slip planes in the crystal structure influences the tableability of the pharmaceutical powders.<sup>20-24</sup> Slip planes are planes with highest molecular density and weak interplanar interactions and can be identified using method described previously.<sup>25</sup> As per published reports,<sup>21, 23</sup> the dislocation of the slip planes under the applied pressure provides a greater bonding area and therefore, a higher plastic deformation can be achieved. EM posses slip plane like system called microstructure that mimics slip plane of single crystal.

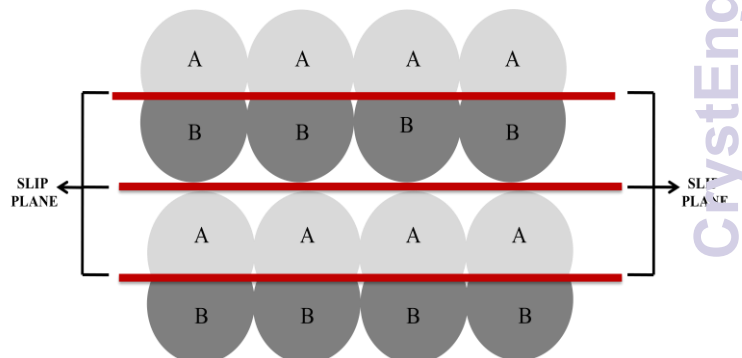


Fig. 11 A schematic diagram showing lamellar growth of a binary eutectic mixture. (EM consists of ASP:PCM in the molar ratio of 1:1)

As depicted in Fig. 11, lamellar microstructure of eutectic system crystallizes out as side by side planes, by the means of couple growth mechanism.<sup>7</sup> These planes are expected to possess the highest intraplanar density and greatest interplanar

spacing, similar to slip planes in the crystal lattice. Hence, it was assumed that the interphase boundary has mechanical implications comparable to slip plane in the single crystals. The greater compressibility and plastic deformation of EM over PM supported this hypothesis. However mechanistic understanding of this requires a detailed examination of eutectic microstructure.

Eutectics possess a microstructure-level periodicity that is different than that of either pure crystalline phase. Without this microstructural element, the system cannot be accurately classified as a eutectic solid.<sup>7</sup> The effective entropy change and the volume fraction of the eutectic phase, during solidification are interrelated and this relationship may be used to characterize the microstructure.<sup>26</sup> The difference in entropy of fusion ( $\Delta S_f$ ) between the individual components controls the resulting eutectic microstructure.<sup>27</sup> When two materials possess equivalent or very similar  $\Delta S_f$  values, both phases grow simultaneously behind a planar solid-liquid interface resulting in a normal eutectic microstructure (Fig. 11), that appears as alternating lamellae or rods of one phase embedded in the other. In contrast, large differences in  $\Delta S_f$  result in faceted growth producing an anomalous structure, which may manifest as one of many internal structures (structural variants).<sup>7</sup>

Another report classified the EM on the basis of entropy of fusion of component as reported in Table 4.<sup>28</sup>

**Table 4.** Classification of EM based on entropies of fusion.

Entropy of fusion	Eutectic mixture
Both component's have low entropies of fusion (<2 J/gK)	Lamellar or rod shape, couple growth
One component has low entropy of fusion (<2 J/gK)	Irregular or regular complex structure
Both component's have high entropies of fusion (>2 J/gK)	Irregular structure no couple growth, grow near each other

In the present investigation, both the components i.e. ASP (0.65 J/gK) and PCM (0.61 J/gK) showed almost similar entropy of fusion, with both values being less than 2 J/gK. Hence, as discussed above, a lamellar microstructure was expected. This was further confirmed by SEM and CLSM. The characteristic pattern of crystallization of the lamellar microstructures has been reported in the literature.<sup>7</sup> Microphotographs of ASP-PCM eutectic system showed similar crystallization pattern, thus confirming formation of lamellar microstructure (Fig. 6). Microstructure, characteristic of eutectic system was not seen in case of individual component.

The lamellar microstructure of EM resulted in incoherent interphase boundaries (the line between the A and B in Fig. 11). This provides thermodynamically stable interface, as compared to the normal coherent interactions that comprise the individual

crystalline phases of ASP and PCM. This boundary possesses a higher free energy because its structural makeup consists of non bonded interactions (NBIs) between different molecules i.e. ASP and PCM.

These interactions are typically not energetically equivalent to those between like molecules. Further, the number of unfulfilled bonds at the interphase boundary is greater relative to either pure component phase, and the NBIs formed between unlike molecules (ASP and PCM) are not as stable relative to those involved in maintaining the pure component crystal lattice, resulting in an increase in internal energy. These bonds are, therefore, energetically easier to overcome.<sup>7</sup>

Thus, lamellar microstructure of ASP-PCM eutectic system can be considered as layered microstructure having weaker interactions between two adjacent layers. Sliding of the adjacent planes over each other under the applied compaction pressure offered higher plastic deformation and hence greater interparticulate bonding area. Heckel analysis was consistent with this and showed the lower mean yield pressure (46.9 MPa) for eutectic system as compared to PM (222.8 MPa), thus confirming the better plastic deformation of EM. According to the standard suggested by Rowe and Roberts for the mechanical classification of pharmaceutical powders<sup>29</sup>, EM can be classified as plastically deforming material whereas PM as a brittle material. This may help to improve the processability and tableting behaviour of the active pharmaceutical ingredients during formulation development.

The CTC profile also revealed that compactibility of both, EM and PM was not significantly different (Fig. 9). As both the powders showed similar particle size distribution and specific surface area, compactibility plots of the two powders represent their relative interparticulate bonding strength. Both, EM and PM exhibited similar tablet tensile strength at a given porosity, thus, indicating similar interparticulate bonding strength of the two materials. However, this was unexpected as interphase boundary of eutectic microstructure exhibits weaker intermolecular interactions.

Sun et al also correlated the melting temperature with interparticulate bonding strength of L-Lysine salts.<sup>30</sup> Here, EM showed lower melting temperature than PM and hence lower interparticulate bonding strength can be expected. Nevertheless, this counterintuitive behaviour of eutectic system is consistent with our recent observation that true density rather than thermodynamic properties like heat of fusion or melting temperature govern the interparticulate bonding strength of pharmaceutical materials.<sup>24,31-34</sup> Authors have studied compaction behaviour of various pharmaceutical polymorphic systems namely, clopidogrel bisulphate forms I and II, indomethacin forms  $\alpha$  and  $\gamma$ , ranitidine hydrochloride forms I and II and clarithromycin forms I and II. In all the systems, polymorph having higher true density showed greater interparticulate bonding strength. In the present study, both, EM (1.371 g/cm<sup>3</sup>) and PM (1.38 g/cm<sup>3</sup>) showed similar true

## ARTICLE

CrystEngComm

density values and exhibited no difference in bonding strength, thus supporting our previous finding.<sup>24, 31-34</sup> However, studies on diverse materials needs to be performed to establish the correlation between true density and interparticulate bonding strength.

### Conclusion

The greater compressibility of EM was attributed to layered microstructure. Sliding of the adjacent layer over each other under applied compaction pressure offered higher plastic deformation and hence greater interparticulate bonding area over PM. Thus, as hypothesized, lamellar microstructure of eutectic system has mechanical implications, that are comparable to the layered crystal structure (slip plane system). Similar interparticulate bonding strength of both the mixtures, despite lower melting temperature of EM, was consistent with our previous reports that correlated bonding strength of the materials to their true density rather than thermodynamic properties.

### References

1. Y. Feng and D. J. Grant, *Pharm. Res.*, 2006, **23**, 1608-1616.
2. C. C. Sun, *J. Adhes. Sci. Technol.*, 2011, **25**, 483-499.
3. K. Chow, H. H. Tong, S. Lum and A. H. Chow, *J. Pharm. Sci.*, 2008, **97**, 2855-2877.
4. R. Rastogi and V. Rastogi, *J. Cryst. Growth.*, 1969, **5**, 345-353.
5. S. Janssens and G. Van den Mooter, *J. Pharm. Pharmacol.*, 2009, **61**, 1571-1586.
6. C. Leuner and J. Dressman, *Eur. J. Pharm. Biopharm.*, 2000, **50**, 47-60.
7. M. D. Moore and P. L. Wildfong, *J. Pharm. Innov.*, 2009, **4**, 36-49.
8. C. Matz, A. Bauer-Brandl, T. Rigassi, R. Schubert and D. Becker, *Drug Dev. Ind. Pharm.*, 1999, **25**, 117-130.
9. K. S. Khomane and A. K. Bansal, *Int. J. Pharm.*, 2013, **455**, 1-4.
10. P. K. More, K. S. Khomane and A. K. Bansal, *Int. J. Pharm.*, 2012, **441**, 527-534.
11. K. Florey, H. G. Brittain, D. J. Mazzo, T. J. Wozniak, G. S. Brenner, G. A. Forcier and A. A. Al-Badr, *Analytical profiles of drug substances and excipients*, Academic press, 1992.
12. *Japan Pat.*, 18,232/66, 1966.
13. P. Mroso, W. Po, A. Li and W. Irwin, *J. Pharm. Sci.*, 1982, **71**, 1096-1101.
14. G. Nichols and C. S. Frampton, *J. Pharm. Sci.*, 1998, **87**, 684-693.
15. A. D. Bond, R. Boese and G. R. Desiraju, *Angew. Chem. Int. Ed.*, 2007, **46**, 618-622.
16. R. Heckel, *Trans. Metall. Soc. AIME*, 1961, **221**, 1001-1008.
17. S. Patel, A. M. Kaushal and A. K. Bansal, *Pharm. Res.*, 2007, **24**, 111-124.
18. R. Heckel, *Trans Metall Soc AIME*, 1961, **221**, 671-675.
19. S. Patel, A. M. Kaushal and A. K. Bansal, *Crit. Rev. Ther. Drug Carrier. Syst.*, 2006, **23**, 1-65.
20. Y. Feng, D. J. Grant and C. C. Sun, *J. Pharm. Sci.*, 2007, **96**, 3324-3333.
21. C. Sun and D. J. Grant, *Pharm. Res.*, 2001, **18**, 274-280.
22. C. C. Sun and D. J. Grant, *Pharm. Res.*, 2004, **21**, 382-386.
23. C. C. Sun and H. Hou, *Cryst. Growth Des.*, 2008, **8**, 1575-1579.
24. P. Upadhyay, K. S. Khomane, L. Kumar and A. K. Bansal, *CrystEngComm*, 2013, **15**, 3959-3964.
25. C. C. Sun and Y. H. Kiang, *J. Pharm. Sci.*, 2008, **97**, 3456-3461.
26. G. Meng, X. Lin and W. Huang, *Mater. Lett.*, 2008, **62**, 984-987.
27. J. Hunt and K. Jackson, *Trans Met Soc AIME*, 1966, **236**, 843-852.
28. M. Taylor, R. Fidler and R. Smith, *Metall. Trans.*, 1971, **2**, 1793-1798.
29. R. Roberts and R. Rowe, *Chem. Eng. Sci.*, 1987, **42**, 903-911.
30. C. Sun and D. J. W. Grant, *Pharm. Res.*, 2001, **18**, 281-286.
31. K. S. Khomane and A. K. Bansal, *AAPS PharmSciTech*, 2013, **14**, 1169-1177.
32. K. S. Khomane and A. K. Bansal, *J. Pharm. Sci.*, 2013, 10.1002/jps.23751.
33. K. S. Khomane, P. K. More and A. K. Bansal, *J. Pharm. Sci.*, 2012, **101**, 2408-2416.
34. K. S. Khomane, P. K. More, G. Raghavendra and A. K. Bansal, *Mol. Pharmaceutics*, 2013, **10**, 631-639.